arXiv:1401.5992v2 [cond-mat.mes-hall] 12 May 2014

Electric dipole induced universality for Dirac fermions in graphene

Alessandro De Martino,[1] Denis Klöpfer,[2] Davron Matrasulov,[3] and Reinhold Egger[2]

[1] *Department of Mathematics, City University London, London EC1V 0HB, United Kingdom*
[2] *Institut für Theoretische Physik, Heinrich-Heine-Universität, D-40225 Düsseldorf, Germany*
[3] *Turin Polytechnic University in Tashkent, 17 Niyazov Str., 100095 Tashkent, Uzbekistan*

(Dated: May 13, 2014)

We study electric dipole effects for massive Dirac fermions in graphene and related materials. The dipole potential accomodates towers of infinitely many bound states exhibiting a universal Efimov-like scaling hierarchy. The dipole moment determines the number of towers, but there is always at least one tower. The corresponding eigenstates show a characteristic angular asymmetry, observable in tunnel spectroscopy. However, charge transport properties inferred from scattering states are highly isotropic.

PACS numbers: 72.80.Vp, 73.22.Pr, 71.15.Rf

Introduction.—Close to the neutrality point, the quasiparticle excitations in a graphene monolayer are two-dimensional (2D) Dirac fermions [1], where a gap Δ can be opened, e.g., by strain engineering [2], spin-orbit coupling [3], strong electron-electron interactions [4], substrate-induced superlattices [5, 6], or in a ribbon geometry [1]. Graphene thus provides experimental access to relativistic quantum effects such as supercriticality, where a Coulomb impurity of charge $Q = Ze$ accomodates bound states that 'dive' into the filled Dirac sea for $Z > Z_c$ [4, 7–14]. While $Z_c \approx 170$ is normally prohibitively large [16, 17], the smaller value $Z_c \approx 1$ in graphene has revealed supercriticality in tunneling spectroscopy [13, 14], where the impurity was created by pushing together charged Co [12] or Ca [14] adatoms with a STM tip. The charge Q of the resulting cluster can be tuned by a local gate voltage. Arranging suitably charged clusters ('nuclei') on graphene, one may then design 'molecules' in an ultrarelativistic regime otherwise unreachable.

Here we predict universal quantum effects, different from supercriticality, for Dirac fermions in the $1/r^2$ *dipole* potential of two oppositely charged ($\pm Q$) nuclei at distance d, with electric dipole moment $p = Qd$. Surprisingly, the Dirac dipole problem has not been discussed so far, presumably because of the lack of heavy anti-nuclei preventing its realization in atomic physics. However, it could be directly studied using STM spectroscopy in graphene [12–14]. A similar $1/r^2$ potential also describes conical singularities [15]. Our main results are as follows, cf. Fig. 1. (i) The spectrum is particle-hole symmetric. Bound states inside the gap, $E = \pm(\Delta - \varepsilon)$ with binding energy $\varepsilon \ll \Delta$, come in (j,κ) towers of definite 'angular' quantum number, $j = 0, 1, 2, \ldots$, and parity $\kappa = \pm$ (with $j + \kappa \geq 0$). The (j,κ) tower is only present if the dipole moment exceeds a critical value, $p > p_{j,\kappa}$, but then contains infinitely many bound states. Since $p_{0,+} = 0$, there is at least one such tower. The lowest-lying finite $p_{j,\kappa}$ are listed in Table I, with excellent agreement between two different derivations. (ii) Bound states in the same tower

Table I. The lowest few finite critical dipole moments, where $p^{\rm M}_{j,\kappa}$ follows from the Mathieu eigenvalues, Eq. (12), and $p^{\rm AK}_{j,\kappa}$ from solving the two-center problem, Eq. (16).

(j,κ)	$p^{\rm M}_{j,\kappa}\Delta$	$p^{\rm AK}_{j,\kappa}\Delta$
$(1,-)$	1.89492	1.88805
$(1,+)$	5.32466	5.32565
$(2,-)$	10.4819	10.4820
$(2,+)$	17.3571	17.3572
$(3,-)$	25.9511	25.9512
$(3,+)$	36.2639	36.2640

obey the scaling hierarchy

$$\frac{\varepsilon_{n+1}}{\varepsilon_n} = e^{-2\pi/s_{j,\kappa}}, \quad n = 1, 2, \ldots \tag{1}$$

where for p close to (but above) $p_{j,\kappa}$,

$$s_{j,\kappa}(p) \simeq \begin{cases} \sqrt{2}p\Delta, & (j,\kappa) = (0,+), \\ \alpha\sqrt{(p - p_{j,\kappa})\Delta}, & j > 0, \end{cases} \tag{2}$$

with $\alpha \approx 0.956$. As $n \to \infty$, all bound states approach one of the gap edges as accumulation point. Equation (1) agrees with the universal Efimov law for the binding energies of three identical bosons with short-ranged particle interactions [18–20]. (iii) Numerical diagonalization of the Dirac equation in a finite disc geometry indicates that as p increases, the bound states approach $E = 0$ without ever reaching it. The absence of zero modes is also shown analytically. (iv) The scattering state for $|E| \gg \Delta$ implies an isotropic transport cross-section, such that charge transport is independent of the angle between current flow and dipole direction.

Model.—We study 2D Dirac fermions with a mass gap Δ. With $\hbar = e = 1$ and Fermi velocity $v = 1$, the Hamiltonian is

$$H = (-i\partial_x)\sigma_x + (-i\partial_y)\sigma_y + \Delta\sigma_z + V. \tag{3}$$

In graphene, the two components of the spinor, $\Psi = (\phi, \chi)^T$, correspond to the two sublattices, where the

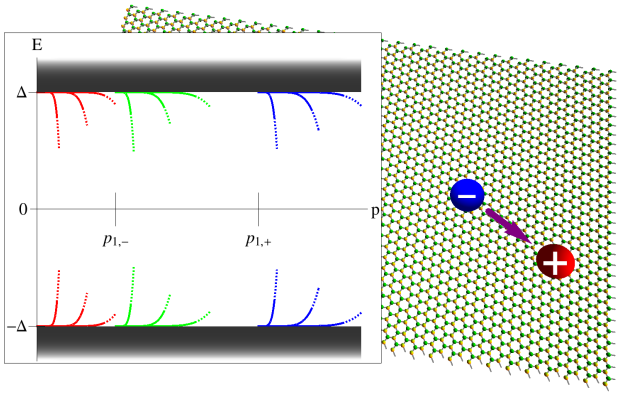

Figure 1. Sketch of the spectrum vs dipole moment p for Dirac fermions with gap Δ in a dipole potential. For $|E| > \Delta$, we have scattering states [Eq. (18)]. Bound states inside the gap are arranged in towers $(j, \kappa = \pm)$. Such a tower exists only when $p > p_{j,\kappa}$, with $p_{0,+} = 0$ and $p_{j>0,\kappa}$ in Table I. Bound states satisfy the Efimov scaling law [Eq. (1)], where both gap edges are accumulation points. The background shows the schematic setup.

Pauli matrices $\sigma_{x,y,z}$ act in this space and we consider a single K point and fixed spin projection [1]. Equation (3) also describes 'molecular graphene' with CO molecules deposited on a copper surface [21], and the surface states of topological insulators like Bi_2Se_3 or Bi_2Te_3 [22]. Assuming two oppositely charged nuclei at $x = \pm d/2$, the potential reads

$$V(x,y) = \frac{p/d}{\sqrt{(x+d/2)^2+y^2}} - \frac{p/d}{\sqrt{(x-d/2)^2+y^2}}, \quad (4)$$

where $p = Qd$ is the dipole moment [23]. For equal charges in the two-center potential (4), similar physics as for a single impurity is found [24]. In polar coordinates the Dirac equation reads

$$\begin{pmatrix} V+\Delta-E & e^{-i\theta}(-i\partial_r - \frac{1}{r}\partial_\theta) \\ e^{i\theta}(-i\partial_r + \frac{1}{r}\partial_\theta) & V-\Delta-E \end{pmatrix} \begin{pmatrix} \phi \\ \chi \end{pmatrix} = 0. \quad (5)$$

Far away from the nuclei, $r \gg d$, Eq. (4) is well approximated by the point-like dipole form

$$V_d(r,\theta) = -\frac{p\cos\theta}{r^2}. \quad (6)$$

The $r \to 0$ singularity implies that Eq. (5) for $V = V_d$ requires regularization to avoid the usual fall-to-the-center problem [25]. To that end one may resort to V in Eq. (4), but simpler regularization schemes are also possible, see below. For nonrelativistic Schrödinger fermions, the dipole captures bound states only above a finite critical dipole moment in three dimensions (3D) [26–30]. However, a dipole binds states for arbitrarily small p in the 2D Schrödinger case [29].

Particle-hole transformation.—The Hamiltonian (3) with V in Eq. (4) is mapped to $UHU^\dagger = -H$ by the unitary transformation $U = \sigma_x \mathcal{R}_x$, with $\mathcal{R}_x$ the reflection $x \to -x$. An eigenstate $\Psi_E(x,y)$ at energy E is mapped to another eigenstate at energy $-E$,

$$\Psi_{-E}(x,y) = U\Psi_E(x,y) = \sigma_x \Psi_E(-x,y). \quad (7)$$

Hence all solutions to Eq (5) come in $\pm E$ pairs. It is then sufficient to study $E > 0$ only, with the $-E$ partner state following from Eq. (7). The dipole moment sign is also irrelevant, and $p > 0$ below.

Near the band edges.—We first consider Eq. (5) for energies close to the band edge, $E = -\Delta + \varepsilon$ with $|\varepsilon| \ll \Delta$, where $\varepsilon > 0$ corresponds to bound states inside the gap and $\varepsilon < 0$ to continuum states. For $p \ll d^2\Delta$, the upper spinor component stays always 'small', $\phi \simeq \frac{1}{2\Delta} e^{-i\theta}\left(i\partial_r + \frac{1}{r}\partial_\theta\right)\chi$, and Eq. (5) leads to an effective Schrödinger equation for the lower spinor component,

$$\left(-\frac{1}{2\Delta}\nabla^2 - V + \varepsilon\right)\chi = 0, \quad (8)$$

with the 2D Laplacian ∇^2. We proceed with the potential $V = V_d$ in Eq. (6), where Eq. (8) is solved by the ansatz $\chi(r,\theta) = R(r)Y(\theta)$. With separation constant γ, the angular function satisfies an ε-independent Mathieu equation,

$$\left(\frac{d^2}{d\theta^2} + \gamma - 2p\Delta\cos\theta\right) Y(\theta) = 0, \quad (9)$$

which admits 2π-periodic solutions only for characteristic values $\gamma = \gamma_{j,\kappa}(p)$, where $\kappa = \pm$ is the parity, i.e., $Y_{j,\kappa}(-\theta) = \kappa Y_{j,\kappa}(\theta)$, and due to the anisotropy, $j = 0, 1, 2, \ldots$ differs from conventional angular momentum, with $j + \kappa \geq 0$. Using standard notation [31, 32], the solutions to Eq. (9) are expressed in terms of Mathieu functions ce_{2j} and se_{2j}, with eigenvalues a_{2j} and b_{2j}, respectively,

$$Y_{j,+}(\theta) = \mathrm{ce}_{2j}\left(\frac{\theta}{2}, 4p\Delta\right), \quad \gamma_{j,+} = \frac{1}{4}a_{2j}(4p\Delta), \quad (10)$$
$$Y_{j,-}(\theta) = \mathrm{se}_{2j}\left(\frac{\theta}{2}, 4p\Delta\right), \quad \gamma_{j,-} = \frac{1}{4}b_{2j}(4p\Delta).$$

The characteristic values are ordered as $\gamma_{0,+} < \gamma_{1,-} < \gamma_{1,+} < \gamma_{2,-} < \ldots$ for given p. With $\gamma = \gamma_{j,\kappa}(p)$, the radial equation reads

$$\left(\frac{d^2}{dr^2} + \frac{1}{r}\frac{d}{dr} - \frac{\gamma}{r^2} - 2\Delta\varepsilon\right) R(r) = 0. \quad (11)$$

To regularize the fall-to-the-center singularity, we impose the Dirichlet condition $R(r_0) = 0$ at a short-distance scale $r_0 \approx d$ [33]. We show below that this regularization does not affect universal spectral properties such as the Efimov law (1).

Efimov scaling.—Let us now look for bound states, $\varepsilon > 0$. The solution of Eq. (11) decaying for $r \to \infty$ is the Macdonald function $K_{\sqrt{\gamma}}\left(\sqrt{2\Delta\varepsilon}\, r\right)$ [31], and $R(r_0) = 0$ then yields an energy quantization condition within each (j,κ) tower. Thereby the binding energies, $\varepsilon_{n,j,\kappa} = z_n^2/(2\Delta r_0^2)$, are expressed in terms of the positive zeroes, $z_1 > z_2 > \ldots > 0$, of $K_{\sqrt{\gamma_{j,\kappa}}}(z)$. Since only $K_{is}(z)$ (with imaginary order) has zeroes [31], bound states require $\gamma_{j,\kappa}(p) < 0$. This condition is satisfied for $p > p_{j,\kappa}$ with

$$\gamma_{j,\kappa}\left(p_{j,\kappa}\right) = 0. \tag{12}$$

The lowest few $p_{j>0,\kappa}$ resulting from Eq. (12) are listed in Table I. With increasing dipole moment, each time that p hits a critical value $p_{j,\kappa}$, a new infinite tower of bound states emerges from the continuum. Since $\gamma_{0,+}(p) < 0$ for all p [32], we find $p_{0,+} = 0$: at least one tower is always present. Explicit binding energies follow from the small-z expansion of $K_{is}(z)$ [31]. With the positive numbers $s_{j,\kappa}(p) = \sqrt{-\gamma_{j,\kappa}(p)}$ for $p > p_{j,\kappa}$, see Eq. (2), we obtain

$$\varepsilon_{n,j,\kappa} = \frac{2}{\Delta r_0^2} e^{\varphi(s_{j,\kappa})} e^{-2\pi n/s_{j,\kappa}}, \tag{13}$$

where $\varphi(s) = (2/s)\,\mathrm{arg}\Gamma(1+is)$. This becomes more and more accurate as n increases. For $n \to \infty$, using particle-hole symmetry, the energies accumulate near both edges, $\varepsilon_n \to 0$. Importantly, Eq. (13) implies the Efimov scaling law announced in Eq. (1). This relation has its origin in the *large-distance* behavior of the dipole potential, and is thus expected to be independent of short-distance regularization issues. A similar behavior has been predicted for the quasi-stationary resonances of a supercritical Coulomb impurity in graphene [9, 10], and for 3D Schrödinger fermions [26, 30].

Tunneling density of states.—The above solution also yields the probability density $|\Psi(r,\theta)|^2$, which is probed by the local tunneling density of states when the energy matches the respective bound state energy, and can be measured in STM spectroscopy experiments [12–14]. Figure 2 shows typical results for the two lowest hole-like radial bound states ($n = 1, 2$) in the $(0,+)$ and $(1,-)$ tower, respectively. The pronounced asymmetry along the x-direction is due to the Mathieu functions in Eq. (10) and is a characteristic feature to look for in experiments. The reflected ($x \to -x$) profile is found for the electron-like partner at energy $+|E|$. The radial distribution comes from the Macdonald function (with $n-1$ nodes at $r > r_0$), which explains the sharp drop from a finite value to almost zero when going outwards from the origin. Finally, because of the proliferation of bound states near the gap edges, the total density of states, $\nu(E)$, becomes singular as $|E|$ approaches Δ from below,

$$\nu(E) \simeq \frac{1}{\Delta - |E|} \sum_{j,\kappa} \Theta(p - p_{j,\kappa}) \frac{s_{j,\kappa}}{2\pi}, \tag{14}$$

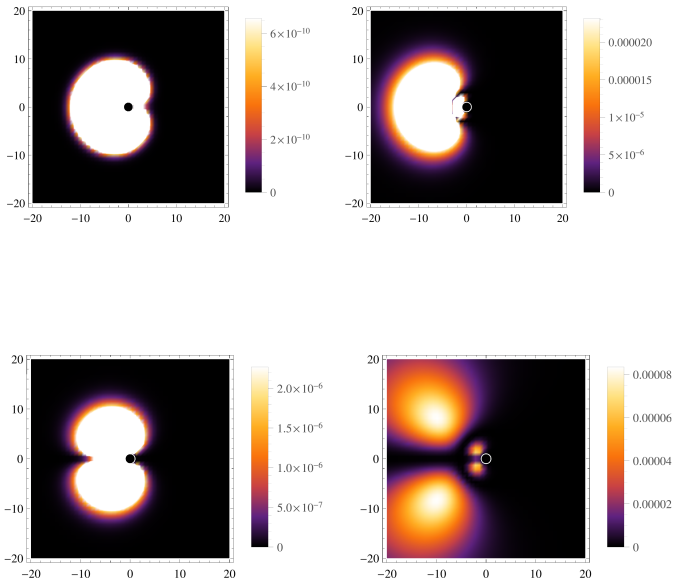

Figure 2. Color-scale plot of $|\Psi(x,y)|^2$, in the x-y plane, where x and y are in units of $r_0 = d/2$, for several bound states with $p\Delta = 5$. For $r < r_0$, the density vanishes due to the Dirichlet condition. The upper part shows the $n = 1$ (left) and the $n = 2$ (right) radial states in the $(0,+)$ tower. The lower part shows the same but for the $(1,-)$ tower.

with the Heaviside step function Θ. Every (j,κ) tower with $p > p_{j,\kappa}$ here contributes to the prefactor through the Efimov exponent $s_{j,\kappa}$ in Eq. (2).

Two-center potential.—Let us now briefly address the two-center potential V in Eq. (4), again for $p \ll d^2\Delta$ and $\varepsilon \ll \Delta$, where the 2D Schrödinger equation (8) applies. Using elliptic coordinates $\xi \geq 1$ and $-1 \leq \eta \leq 1$ [31], where $V(\xi,\eta) = 4p\eta/[(\xi^2-\eta^2)d^2]$, the problem separates with the ansatz $\chi(\xi,\eta) = \frac{Y(\eta)}{(1-\eta^2)^{1/4}} \frac{R(\xi)}{(\xi^2-1)^{1/4}}$. With the separation constant $A = -\gamma + 1/4$, the 'angular' and 'radial' equations, resp.,

$$\left(\frac{d^2}{d\eta^2} + \frac{2p\Delta\eta - A}{1-\eta^2} + \frac{3/4}{(1-\eta^2)^2} - \frac{\varepsilon\Delta d^2}{2}\right) Y(\eta) = 0,$$
$$\left(\frac{d^2}{d\xi^2} + \frac{A}{\xi^2-1} + \frac{3/4}{(\xi^2-1)^2} - \frac{\varepsilon\Delta d^2}{2}\right) R(\xi) = 0, \tag{15}$$

coincide with the Abramov-Komarov equations for the 3D Schrödinger problem [26]. Adapting their analysis for $p\Delta \gg 1$, we find $\gamma < 0$ for $p > p_{j,\kappa}^{\mathrm{AK}}$ with

$$p_{j,\kappa}^{\mathrm{AK}}\Delta = \frac{\Gamma^4(1/4)}{64\pi}\left[\left(2j + \frac{\kappa}{2}\right)^2 - \frac{1}{6\pi}\right], \tag{16}$$

where j and κ take the same values as above. By construction, Eq. (16) is highly accurate for $p\Delta \gg 1$, but

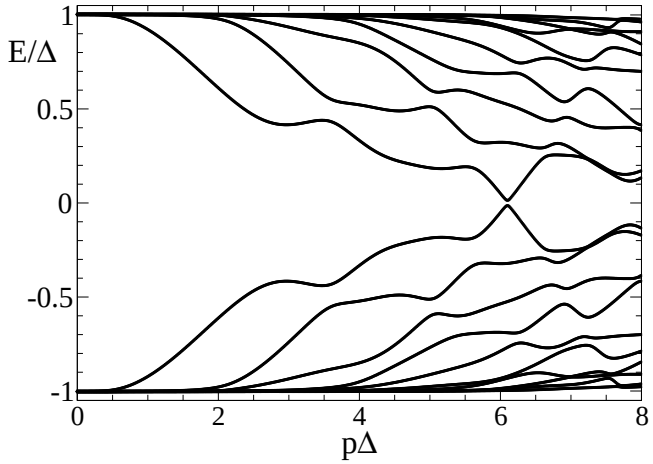

Figure 3. Bound state spectrum vs dipole moment for a circular graphene flake with radius $R_{\rm fl} = 75r_0$, where $r_0 = d/2$, from exact diagonalization of Eq. (5) with infinite-mass boundary conditions at $r = R_{\rm fl}$.

Table I demonstrates that it works very well even for $p\Delta \approx 1.9$. Not surprisingly, the exact result $p_{0,+} = 0$ is not captured by this approach, $p_{0,+}^{\rm AK}\Delta \simeq 0.17$. However, $p_{0,+} = 0$ follows from an exact calculation for the two-center potential [29]. Interestingly, Eq. (16) also provides an analytical approximation for the zeroes of the Mathieu characteristic values. Solving Eq. (15) as in Ref. [26], we recover the spectrum in Eq. (13) with $s_{j,\kappa}$ in Eq. (2), where $\alpha = 4\pi/\Gamma^2(1/4)$ and $r_0 \to d/4$. While apart from the $(0,+)$ tower, bound state energies are obtained in accurate analytical form, $|\Psi(x,y)|^2$ is given only implicitly and thus difficult to extract. Finally, the excellent agreement with the point dipole result confirms that short-distance regularization issues are irrelevant.

Numerical diagonalization.—Since finite-size effects can be important in practice, we have studied the bound-state spectrum for a circular graphene flake of radius $R_{\rm fl} \gg d$, using the full Dirac equation (5) for the point dipole in Eq. (6) [34]. We impose infinite-mass boundary conditions [35] at $r = R_{\rm fl}$, which is consistent with the particle-hole symmetry [Eq. (7)] and allows us to compute the spectrum by exact diagonalization, see Fig. 3. For the value of $R_{\rm fl}$ chosen in Fig. 3, Efimov scaling is not yet fully developed, but the observed spectrum shows the emergence of new bound state towers as the dipole moment increases. Figure 3 also clarifies the fate of bound states upon increasing the dipole moment. First, we find that bound states do not dive into the continuum. This agrees with our analytical results, which are exact close to the gap edges, and indicates that supercriticality is unlikely to occur. Second, with increasing p, bound state energies tend to approach (without ever reaching) zero energy. In fact, the absence of midgap ($E = 0$) states can be explained as follows: Equation (7) implies that a putative zero mode must be of the form $\Psi_{E=0}(r,\theta) = (\psi(r,\theta), \pm\psi(r,\pi-\theta))^T$, with a function $\psi(r,\theta)$. Choosing the + sign (the same follows with the − sign) and $\Delta \to 0$, the Dirac equation (5) reduces to

$$\frac{p\cos\theta}{r^2}\psi(r,\pi-\theta) + e^{i\theta}\left(i\partial_r - \frac{1}{r}\partial_\theta\right)\psi(r,\theta) = 0. \quad (17)$$

The radial dependence is solved by $\psi \sim e^{i(p/r)y(\theta)}$, with an angular function $y(\theta) = y(\pi-\theta)$. However, the resulting equation for $y(\theta)$ does not admit a solution. We conclude that zero modes, given their absence for $\Delta \to 0$, are unlikely to exist for finite Δ [36].

Scattering states.—Finally, we turn to continuum solutions of the Dirac equation with V in Eq. (4). For simplicity, we consider $|E| \gg \Delta$, where the Born approximation [7, 37] is applicable. For an incoming plane wave with momentum $\mathbf{k}$ and $\sigma = {\rm sgn}(E) = \pm$, the asymptotic scattering state is [7]

$$\Psi_{\mathbf{k},\sigma}(r,\theta) \simeq e^{i\mathbf{k}\cdot\mathbf{r}}U_{\mathbf{k},\sigma} + f(\theta,\phi_{\mathbf{k}})\frac{e^{ikr}}{\sqrt{-ir}}U_{\mathbf{k}',\sigma}, \quad (18)$$

with $\mathbf{k}' = k\hat{\mathbf{r}}$, $\phi_{\mathbf{k}}$ the angle between $\mathbf{k}$ and the dipole (x-)axis, and $U_{\mathbf{k},\sigma} = \frac{1}{\sqrt{2}}\begin{pmatrix} e^{-i\phi_{\mathbf{k}}/2} \\ \sigma e^{i\phi_{\mathbf{k}}/2}\end{pmatrix}$. For long wavelengths, $kd \ll 1$, the scattering amplitude is

$$f(\theta,\phi_{\mathbf{k}}) \simeq ip\sqrt{2\pi k}\cos[(\theta-\phi_{\mathbf{k}})/2]\sin[(\theta+\phi_{\mathbf{k}})/2]. \quad (19)$$

The transport and total cross-sections, $\Lambda_{\rm tr} = \int d\theta[1-\cos(\theta-\phi_{\mathbf{k}})]|f(\theta)|^2$ and $\Lambda = \int d\theta|f(\theta)|^2$ [7], resp., are then given by $\Lambda_{\rm tr} = \frac{\pi^2}{2}p^2k$ and $\Lambda = \left(1+2\sin^2\phi_{\mathbf{k}}\right)\Lambda_{\rm tr}$. Remarkably, $\Lambda_{\rm tr}$ is independent of $\phi_{\mathbf{k}}$, with the dipole-induced angular dependence precisely compensated by the $\cos[(\theta-\phi_{\mathbf{k}})/2]$ factor in Eq. (19). This factor is specific for Dirac fermions and causes the well-known 'absence of backscattering' by short-ranged impurities [1]. We then expect the electrical conductivity of a graphene sample containing oriented dipoles to be *isotropic*.

Conclusions.—The electric dipole problem for 2D Dirac fermions exhibits rich physics that could be probed by STM spectroscopy in graphene. The Efimov-like scaling of the bound state energies, with the gap edges as accumulation points, suggests that electrons can be captured (and thus confined) by a dipole potential. This scaling property, formally identical to the scaling of the three-body levels of identical bosons, here emerges in a different physical setting and can be traced to the $1/r^2$ dependence of the dipole potential. While we have disregarded electron-electron interactions beyond a Fermi velocity renormalization [4], Δ tends to suppress charge fluctuations and no profound changes are expected for weak interactions. Future work should clarify whether multi-electron bound states are possible in such a setting.

Acknowledgments.—We thank A. Altland, E. Andrei, H. Siedentop, and A. Zazunov for discussions, and the

DFG (SFB TR12 and SPP 1459) and the Volkswagen-Stiftung for financial support.

[1] A.H. Castro Neto, F. Guinea, N.M.R. Peres, K.S. Novoselov, and A. Geim, Rev. Mod. Phys. **81**, 109 (2009).

[2] M.A.H. Vozmediano, M.I. Katsnelson, and F. Guinea, Phys. Rep. **496**, 109 (2010).

[3] D. Huertas-Hernando, F. Guinea, and A. Brataas, Phys. Rev. B **74**, 155426 (2006).

[4] V.N. Kotov, B. Uchoa, V.M. Pereira, A.H. Castro Neto, and F. Guinea, Rev. Mod. Phys. **84**, 1067 (2012).

[5] L.A. Ponomarenko, R.V. Gorbachev, G.L. Yu, D.C. Elias, R. Jalil, A.A. Patel, A. Mishchenko, A.S. Mayorov, C.R. Woods, J.R. Wallbank, M. Mucha-Kruczynski, B.A. Piot, M. Potemski, I.V. Grigorieva, K.S. Novoselov, F. Guinea, V.I. Fal'ko, and A.K. Geim, Nature (London) **497**, 594 (2013).

[6] J.C.W. Song, A.V. Shytov, and L.S. Levitov, Phys. Rev. Lett. **111**, 266801 (2013).

[7] D.S. Novikov, Phys. Rev. B **76**, 245435 (2007).

[8] V.M. Pereira, J. Nilsson, and A.H. Castro Neto, Phys. Rev. Lett. **99**, 166802 (2007).

[9] A.V. Shytov, M.I. Katsnelson, and L.S. Levitov, Phys. Rev. Lett. **99**, 246802 (2007).

[10] O.V. Gamayun, E.V. Gorbar, and V.P. Gusynin, Phys. Rev. B **80**, 165429 (2009).

[11] D. Klöpfer, A. De Martino, and R. Egger, Crystals **3**, 14 (2013).

[12] Y. Wang, V.W. Brar, A.V. Shytov, Q. Wu, W. Regan, H.-Z. Tsai, A. Zettl, L.S. Levitov, and M.F. Crommie, Nat. Phys. **8**, 653 (2012).

[13] A. Luican-Mayer, M. Kharitonov, G. Li, C.P. Lu, I. Skachko, A.M.B. Goncalves, K. Watanabe, T. Taniguchi, and E.Y. Andrei, Phys. Rev. Lett. **112**, 036804 (2014).

[14] Y. Wang, D. Wong, A.V. Shytov, V.W. Brar, S. Choi, Q. Wu, H.-Z. Tsai, W. Regan, A. Zettl, R.K. Kawakami, S.G. Louie, L.S. Levitov, and M.F. Crommie, Science **340**, 734 (2013).

[15] V.M. Pereira, A.H. Castro Neto, H.Y. Liang, and L. Mahadevan, Phys. Rev. Lett. **105**, 156603 (2010).

[16] W. Greiner, B. Müller, and J. Rafelski, *Quantum electrodynamics of Strong Fields* (Springer, Berlin, 1985).

[17] V.S. Popov, Phys. At. Nucl. **64**, 367 (2001).

[18] V. Efimov, Phys. Lett. B **33**, 563 (1970).

[19] E. Braaten and H.W. Hammer, Phys. Rep. **428**, 259 (2007).

[20] A.O. Gogolin, C. Mora, and R. Egger, Phys. Rev. Lett. **100**, 140404 (2008).

[21] K.K. Gomes, W. Mar, W. Ko, F. Guinea, and H.C. Manoharan, Nature (London) **483**, 306 (2012).

[22] M.Z. Hasan and C.L. Kane, Rev. Mod. Phys. **82**, 3045 (2010).

[23] A substrate dielectric constant can be included by renormalization of p. The potential (6) also arises by deposition of a polar molecule.

[24] O.O. Sobol, E.V. Gorbar, and V.P. Gusynin, Phys. Rev. B **88**, 205116 (2013).

[25] A.A. Perelomov and V.S. Popov, Theor. Math. Phys. **4**, 664 (1970).

[26] D.I. Abramov and I.V. Komarov, Theor. Math. Phys. **13**, 209 (1972).

[27] D.U. Matrasulov, V.I. Matveev, and M.M. Musakhanov, Phys. Rev. A **60**, 4140 (1999).

[28] H.E. Camblong, L.N. Epele, H. Fanchiotti, and C.A.G. Canal, Phys. Rev. Lett. **87**, 220402 (2001).

[29] K. Connolly and D.J. Griffiths, Am. J. Phys. **75**, 527 (2007).

[30] D. Schumayer, B.P. Zyl, R.K. Bhadure, and D.A.W. Hutchinson, EPL **89**, 13001 (2010).

[31] I.S. Gradshteyn and I.M. Ryzhik, *Table of Integrals, Series, and Products* (Academic Press, Elsevier, 2007).

[32] M. Abramowitz and I.A. Stegun (eds.), *Handbook of Mathematical Functions* (Dover, New York, 1965).

[33] On the level of the Dirac equation, this corresponds to vanishing radial current at $r = r_0$.

[34] In the numerics, we use the regularization $V(r < r_0) = -p\cos(\theta)/r_0^2$.

[35] M.V. Berry and R.J. Mondragon, Proc. R. Soc. London A **412**, 53 (1987).

[36] For finite Δ, the squared Dirac equation for $E = 0$ does not contain terms $\propto 1/r^2$ for $r \to \infty$, but at most terms $\propto 1/r^3$ which do not allow for bound states.

[37] A. Zazunov, A. Kundu, A. Hütten, and R. Egger, Phys. Rev. B **82**, 155431 (2010).